



Single-cell RNA sequencing reveals that the immunosuppression landscape induced by chronic stress promotes colorectal cancer metastasis

Yingru Zhang^a, Ying Feng^b, Yiyang Zhao^a, Yuanyuan Feng^a, Mengyao Li^a, Wenkai Wang^a, Zhongya Ni^a, Huirong Zhu^a, Yan Wang^{a,*}

^a Department of Medical Oncology, Shuguang Hospital, Shanghai University of Traditional Chinese Medicine, Shanghai, 201203, China

^b Academy of Integrative Medicine, Shanghai University of Traditional Chinese Medicine, Shanghai, 201203, China

ARTICLE INFO

Keywords:

Chronic stress
Depression
Colorectal cancer
Metastasis
Tumour immune microenvironment
Single-cell RNA seq

ABSTRACT

The high prevalence of depressive disorders in individuals with cancer and their contribution to tumour progression is a topic that is gradually gaining attention. Recent evidence has shown that there are prominent connections between immune gene variants and mood disorders. The homeostasis of the tumour immune microenvironment (TIME) and the infiltration and activation of immune cells play a very important role in the antitumour effect. In this study, we established a compound mouse model with chronic unpredictable mild stress (CUMS) and orthotopic colorectal cancer to simulate colorectal cancer (CRC) patients with depression. Using 10×Genomics single-cell transcriptome sequencing technology, we profiled nearly 30,000 cells from tumour samples of 8 mice from the control and CUMS groups, revealed that immune cells in tumours under a chronic stress state trend toward a more immunosuppressive and exhaustive status, and described the crosstalk between the overall inflammatory environment and immunosuppressive landscape to provide mechanistic information or efficacious strategies for immune-oncology treatments in CRC with depressive disorders.

1. Introduction

Due to the younger age of cancer onset and the ageing of the world's population, the number of cancer survivors has grown dramatically. People who live with cancers need better quality of life while undergoing surgery, chemotherapy, radiotherapy, immunotherapy and other treatments [1]. It is well known that many risk factors promote tumour progression, such as nutrition, obesity, dietary habits, and lifestyle factors [2–4]. Among these factors, the mental health concerns of cancer patients are receiving more attention [5,6]. A pioneering study arranged CRC survivors into clusters by four emotion regulation patterns and suggested that health care professionals should be aware of the individual differences in the emotions of these CRC patients [7]. Our previous randomized controlled clinical study in CRC showed that disease-free survival was negatively correlated with worse emotional function [8].

Depression is one of the most common negative emotions in cancer patients [9], and meta-analyses have reasonably suggested that it might be an independent risk factor in pancancer that is associated with worse survival [10,11]. Moreover, cancer survivors may

* Corresponding author.

E-mail address: yanwang@shutcm.edu.cn (Y. Wang).

<https://doi.org/10.1016/j.heliyon.2023.e23552>

Received 26 April 2023; Received in revised form 6 December 2023; Accepted 6 December 2023

Available online 10 December 2023

2405-8440/© 2023 Published by Elsevier Ltd.

This is an open access article under the CC BY-NC-ND license

(<http://creativecommons.org/licenses/by-nc-nd/4.0/>).

suffer serious side effects from chemotherapy and other treatments that contribute to the development of depressive symptoms [12]. Negative emotions or long-term psychological stress can have adverse consequences for the body, including hormone secretion disorders, immune dysfunction, peripheral nervous system alterations and interactions [13–15], impair the ability of immune cells to secrete cytokines to kill cancer cells, and promote tumour metastasis [16,17]. However, despite the negative impact of chronic stress on people with cancer, the exact mechanisms remain unclear.

In recent years, the development of single-cell RNA sequencing technology has opened up new possibilities at the genetic level for further research to address biological and medical questions, especially in the field of immunology [18]. In this work, we established CUMS-induced depression CRC tumour-bearing mice to uncover a landscape of chronic stress-induced immunosuppression by single-cell RNA sequencing technology to provide strategies for studying the mechanisms by which negative emotion promotes CRC progression.

2. Results

2.1. CUMS-induced depression promotes CRC progression

As shown in Fig. 1A, we established the in situ model of CRC, accompanied by CUMS-induced depression. The open field test, tail suspension test, and forced swimming test verified that the CUMS group mice were depressed before they were sacrificed (Fig. 1B–D). According to the statistics of the survival period of each mouse, the CUMS group was obviously shorter than the control, showing a worse prognosis (Fig. 1E). From the 14th day, the weight of the mice was recorded once every 2 days, and the weight of the CUMS mice was significantly lower than that of the control (Fig. 1F). After two months, metastases were observed in the livers and lungs of the CUMS group mice but were hardly found in the control group (Fig. 1G and H). These results suggest that depression is associated with CRC metastasis and a worse prognosis.

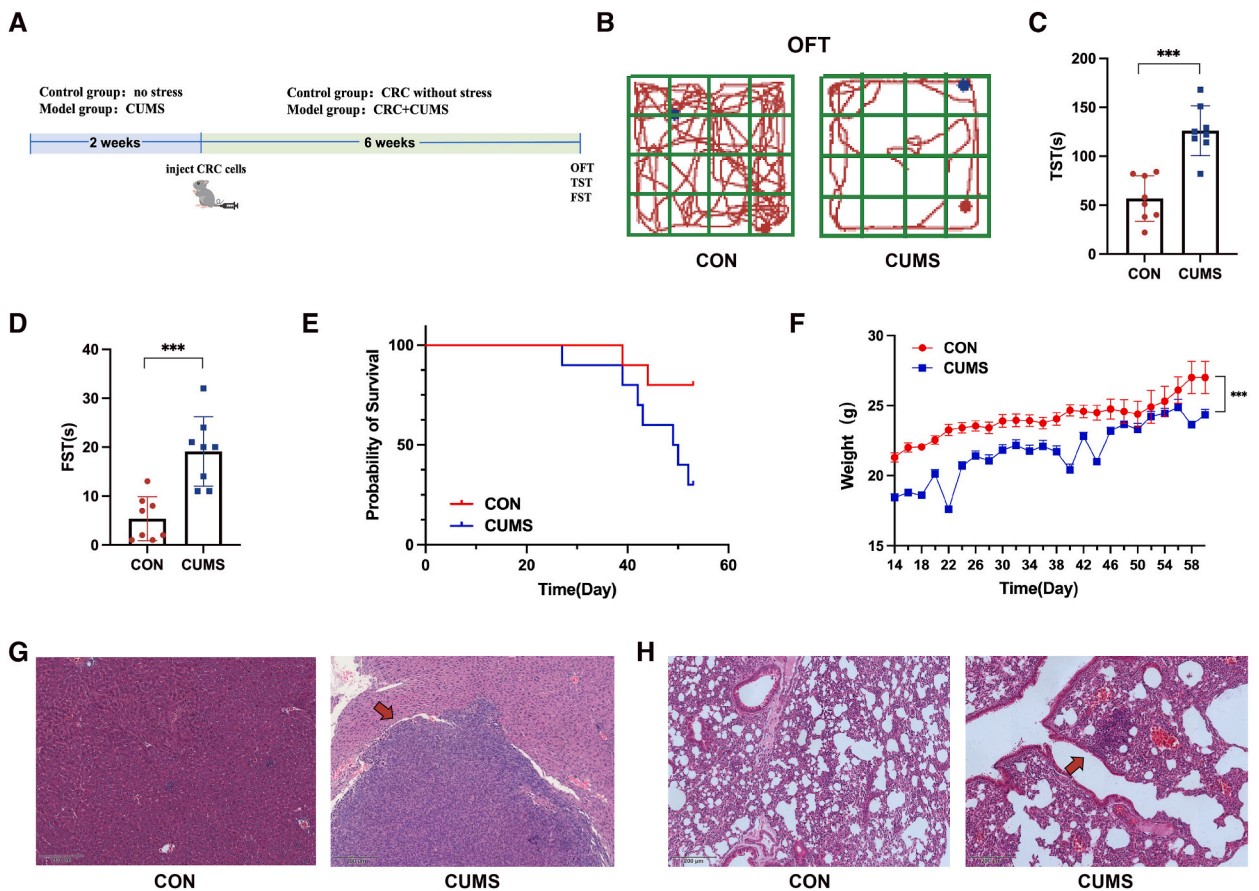


Fig. 1. CUMS-induced depression promotes CRC development. (A) Workflow of depression combined with CRC mouse model. (B) Evaluation by the open field test. (C) Evaluation by tail suspension test (***p* < 0.001). (D) Evaluation by the forced swim test (***p* < 0.001). (E) Survival period of the mice. (F) Body weights of the mice (***p* < 0.001). (G) Histological analysis of livers. (H) Histological analysis of lungs.

2.2. Single-cell RNA sequencing of the in situ CRC in depression mice

To investigate the metergasis of the TIME in tumour progression under chronic stress, we used single-cell RNA-seq to map the tumour-immune transcriptional landscape of four tumours in each group (Fig. 2A). To define major cell populations, we performed unsupervised clustering analysis after gene quantitative quality control on integrated single-cell datasets from control and CUMS tumours. Preliminarily, 19 unique cell clusters, including malignant cells (Clusters 3, 6–8, 10, 12, and 13), macrophages (Clusters 1, 4,

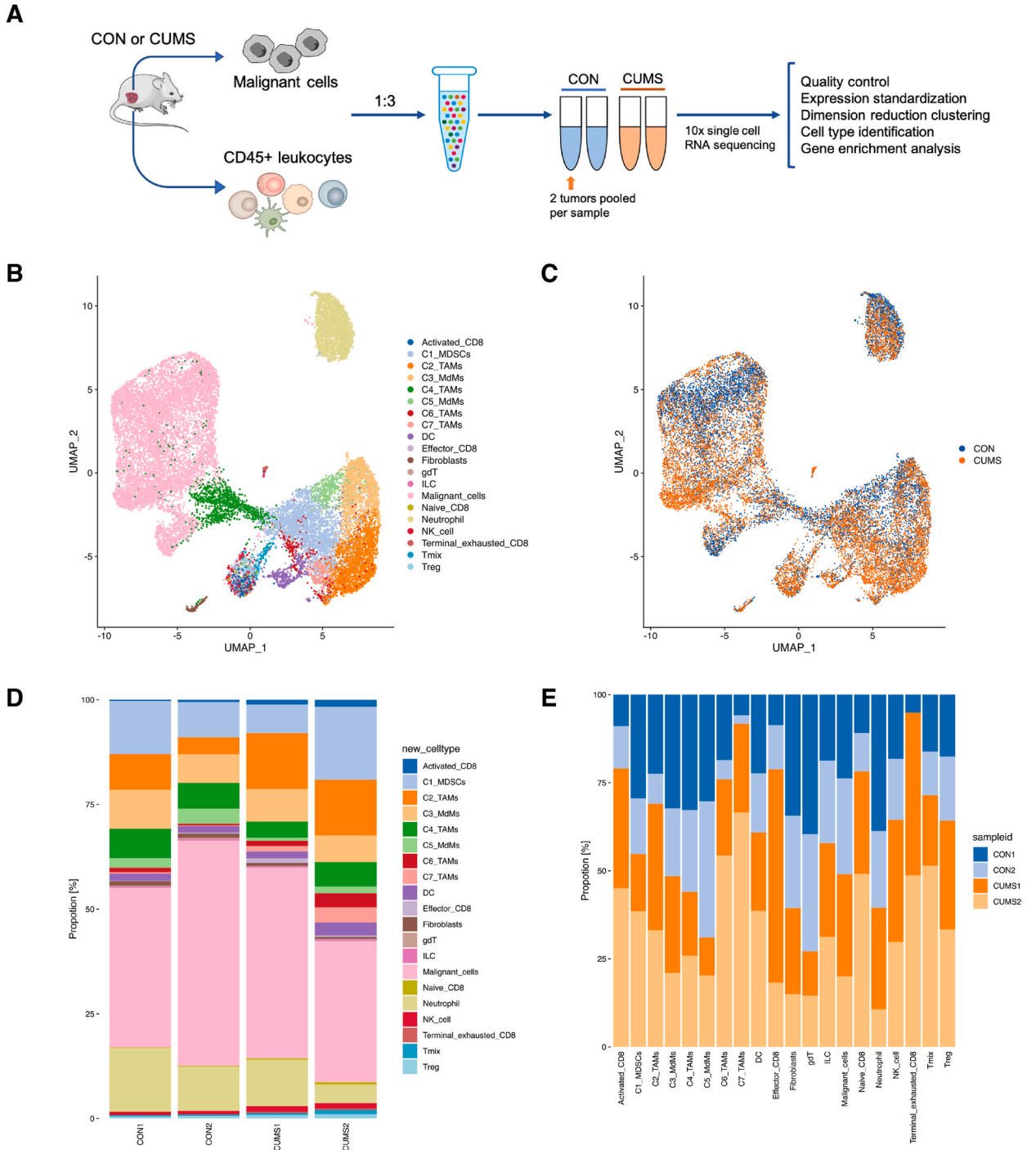


Fig. 2. Single-cell expression map in CRC. (A) Workflow of single-cell RNA-seq. (B) U-MAP visualization of cell clusters. (C) U-MAP visualization of the control and CUMS groups. (D) The proportion of clusters in all cells of each sample. (E) The proportion of each sample in different clusters.

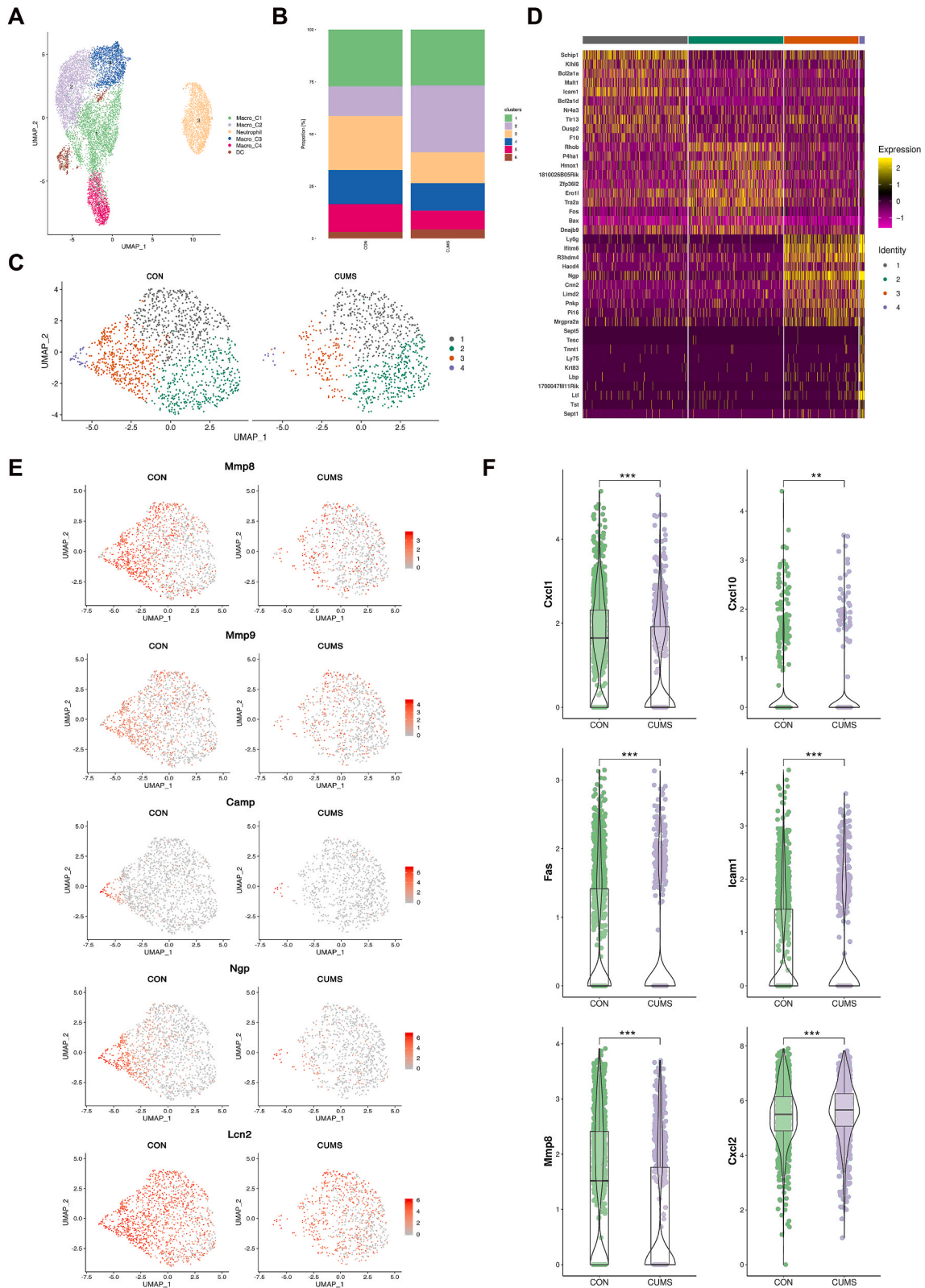
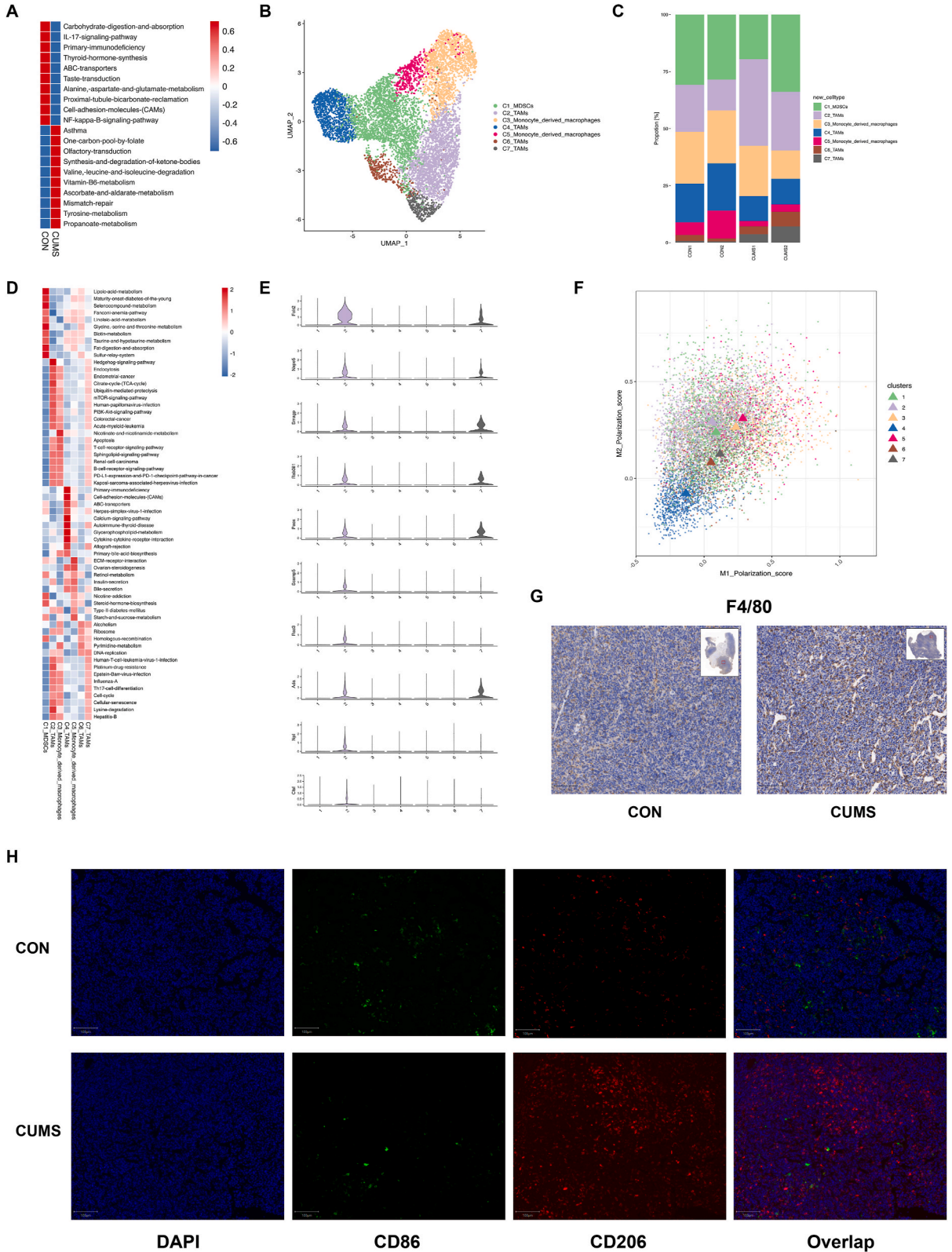


Fig. 3. Analysis of neutrophils. (A) U-MAP visualization of myeloid cells. **(B)** The cluster proportions of myeloid cells in the control and CUMS groups. **(C)** U-MAP visualization of neutrophils in the two groups. **(D)** Marker genes for neutrophil subsets. **(E)** Marker genes for MMP8-neutrophils. **(F)** Differential genes of the two groups in neutrophil subset Cluster 3 (** $p < 0.01$; *** $p < 0.001$).



(caption on next page)

Fig. 4. Analysis of macrophages. (A) GSVA enrichment analysis of macrophages between the control and CUMS groups. (B) U-MAP visualization of macrophages in the two groups. (C) The cluster proportions of macrophages in each sample. (D) GSVA_KEGG enrichment analysis of each cluster in macrophages. (E) Marker genes of C2_TAMs. (F) M1 and M2 scores for each macrophage subset. (G) Histological staining of F4/80 (marker of macrophages). (H) Histological staining of M1 macrophages (CD86, green) and M2 macrophages (CD206, red).

5, 9, and 14–16), T/NK cells (Clusters 11 and 19), neutrophils (Cluster 2), dendritic cells (Cluster 17), and fibroblasts (Cluster 18), were defined by genetic markers (Fig. S1). Furthermore, we categorized these cell clusters into 20 subpopulations (Fig. 2B), and UMAP (nonlinear dimensionality reduction) showed different distributions between the two groups (Fig. 2C). Immune cells from the control group and CUMS group revealed different proportions, in which T-cell and TAM clusters showed significant heterogeneity (Fig. 2D and E).

2.3. Heterogeneity of myeloid cells between CUMS and control CRC

Leukocytes are divided into lymphocytes and myeloid cells according to their origin [19]. In myeloid cells, three cell classes, including six populations, were identified (Fig. 3A), and the proportions of neutrophils and macrophages were significantly different between the two groups (Fig. 3B). Studies have demonstrated that neutrophil infiltration is associated with a better prognosis in the early stages of CRC and could enhance the antitumour immunity of CD8⁺ T cells [20,21]. The decreased proportion of neutrophils in the CUMS group compared with the control group also suggested immunosuppression. In recent years, many scientists have pointed out that tumour-associated neutrophils (TANs) have phenotypic and functional plasticity in the TIME [22]. We used single-cell sequencing technology to perform dimensionality reduction clustering of cells and identified marker genes of each subset by the FindAllMarkers function (test. use = bimod) in Seurat [23] (Fig. 3C and D). Cluster 4, with the genic markers MMP8, MMP9, CAMP, NGP, LCN2, and CXCL8, was named MMP8⁺ TAN and recognized as the ‘antitumour subpopulation’ [24], which was significantly decreased in the CUMS group (Fig. 3E). Of note, the proportion of Cluster 3 characterized by Ly6g, Ifitm6, ngp, and R3hdm4, which was also reduced in the CUMS group, expressed lower CXCL1, CXCL10, FAS, ICAM-1, MMP8 and higher CXCL2 levels than the control

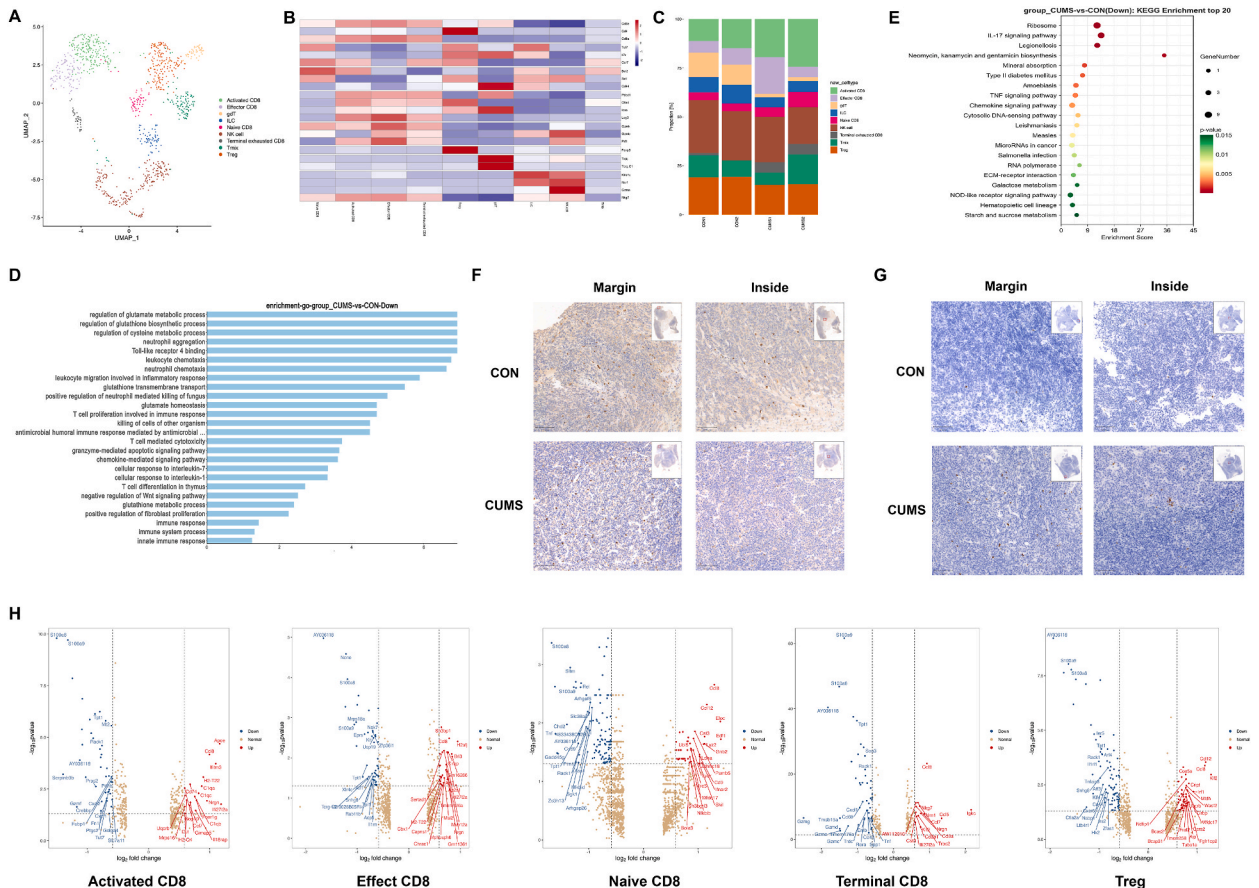


Fig. 5. Analysis of T cells. (A) U-MAP visualization of lymphocytes. (B) Marker genes of lymphocyte subsets. (C) The cluster proportions of lymphocytes in each sample. (D) GO enrichment analysis of activated CD8⁺ T cells. (E) KEGG enrichment analysis of effector CD8⁺ T cells. (F-G) Histological staining of CD8 and CD4. (H) Differential genes in each T-cell subset.

(Fig. 3F).

The GSVA enrichment analysis of macrophages between the two groups showed that the enrichment of the IL-17 pathway and NF- κ B pathway, which are related to the inflammatory response, was significantly reduced (Fig. 4A). Furthermore, the macrophage population was categorized into seven clusters, including myeloid-derived suppressor cells (MDSCs), two clusters of monocyte-derived macrophages and TAMs (Fig. 4B), and among them, TAM populations exhibited a significant difference in proportion between the two groups (Fig. 4C). Then, we used the addmodule score function in Seurat to calculate the expression of each program at the single-cell level. All analysed features were binned based on mean expression, and control features were randomly selected from each bin. Gene sets associated with the above are listed in Table S1. The results suggested that the C2_TAMs with high expression of Fcrl2, Nlpe5, Smagp, Rab31l1, Paox, Scamp5, Rac3, Ada, Npl, and Ctsf genes tend to exhibit the M2 subtype (Fig. 4E and F), and gene enrichment analysis also verified that the cluster was positively related to CRC as well the signalling activity of the PI3K/Akt/mTOR pathway, which plays a propulsive role in the progression of CRC. Moreover, the C2_TAMs with an increased proportion in the CUMS group induced high PD-L1 expression and upregulated the PD-1 checkpoint pathway in cancer (Fig. 4D). These findings were also confirmed by immunohistochemistry and immunofluorescence. In the CUMS group, the expression of macrophage marker proteins was higher than that in the control group (Fig. 4G), and there was a higher frequency of M2 macrophage (CD206) infiltration in CUMS group tumours (Fig. 4H).

2.4. The heterogeneity of lymphocytes between CUMS and control CRC

In lymphocytes, nine populations, including Activated CD8+T cells, Effector CD8+T cells, Naive CD8+T cells, Terminal exhausted CD8+T cells, ILC, Treg, gdT ($\gamma\delta$ T), Tmix, and NK cells (Fig. 5A), whose markers are shown in Fig. 5B were identified, and Fig. 8B shows the correlation between them. Fig. 5C shows a significantly increased proportion of activated CD8+, effector CD8+ and terminal exhausted CD8+ T cells and a significantly decreased proportion of gdT cells. It is worth noting that while the proportion of activated CD8+ T cells increased in CUMS group tumours, their antitumour ability weakened and was associated with a high inflammatory niche. GO enrichment analysis showed that downregulated genes were involved in neutrophil aggregation, leukocyte and neutrophil chemotaxis, T-cell proliferation involved in the immune response, T-cell-mediated cytotoxicity and glutamate metabolism, which is correlated with immune function and depression [25] (Fig. 5D). Upregulated genes were involved in the regulation of behavioural fear response, innate immune response, negative regulation of T-cell differentiation, MHC class II (active CD4+T cells) protein binding and some proinflammatory cytokine pathways (IL-18, IL-6, IL-10, IL-4, IL-2, IL-1), and positive regulation of NF- κ B transcription factor

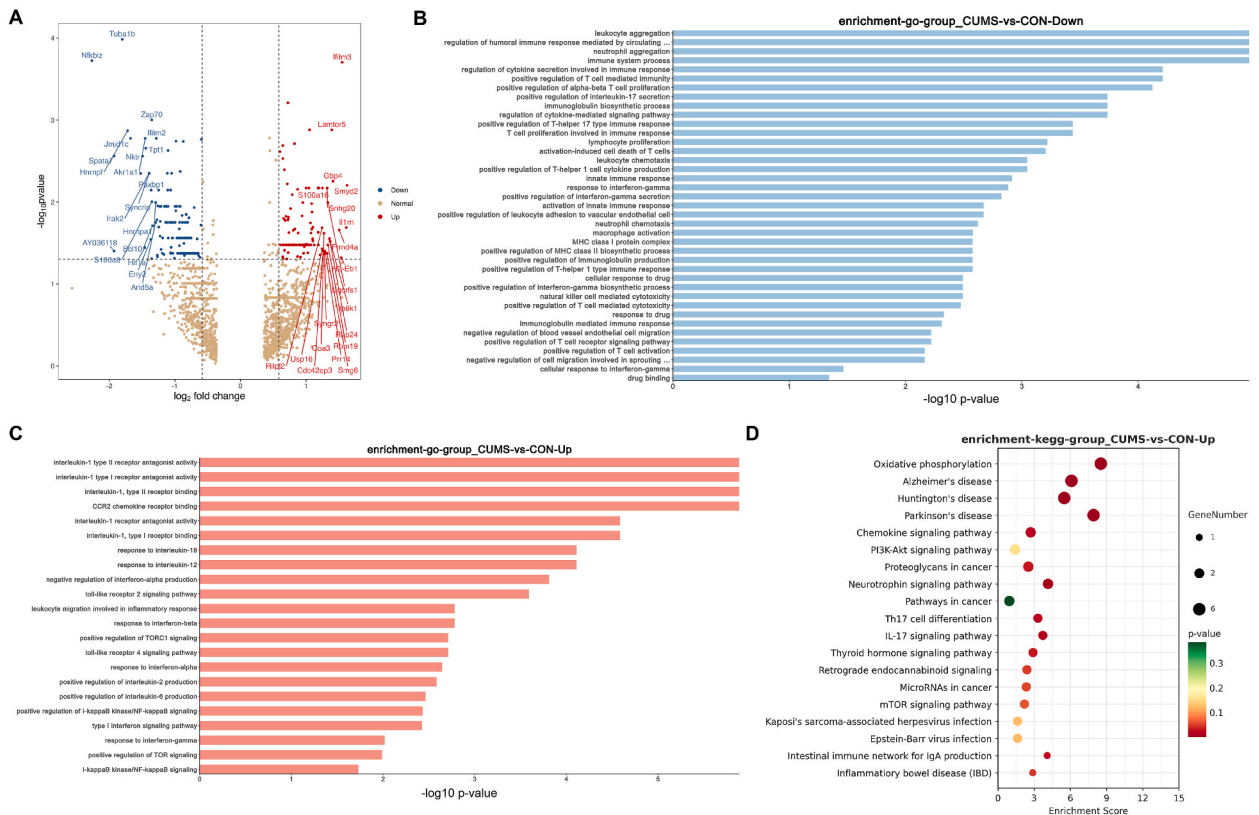
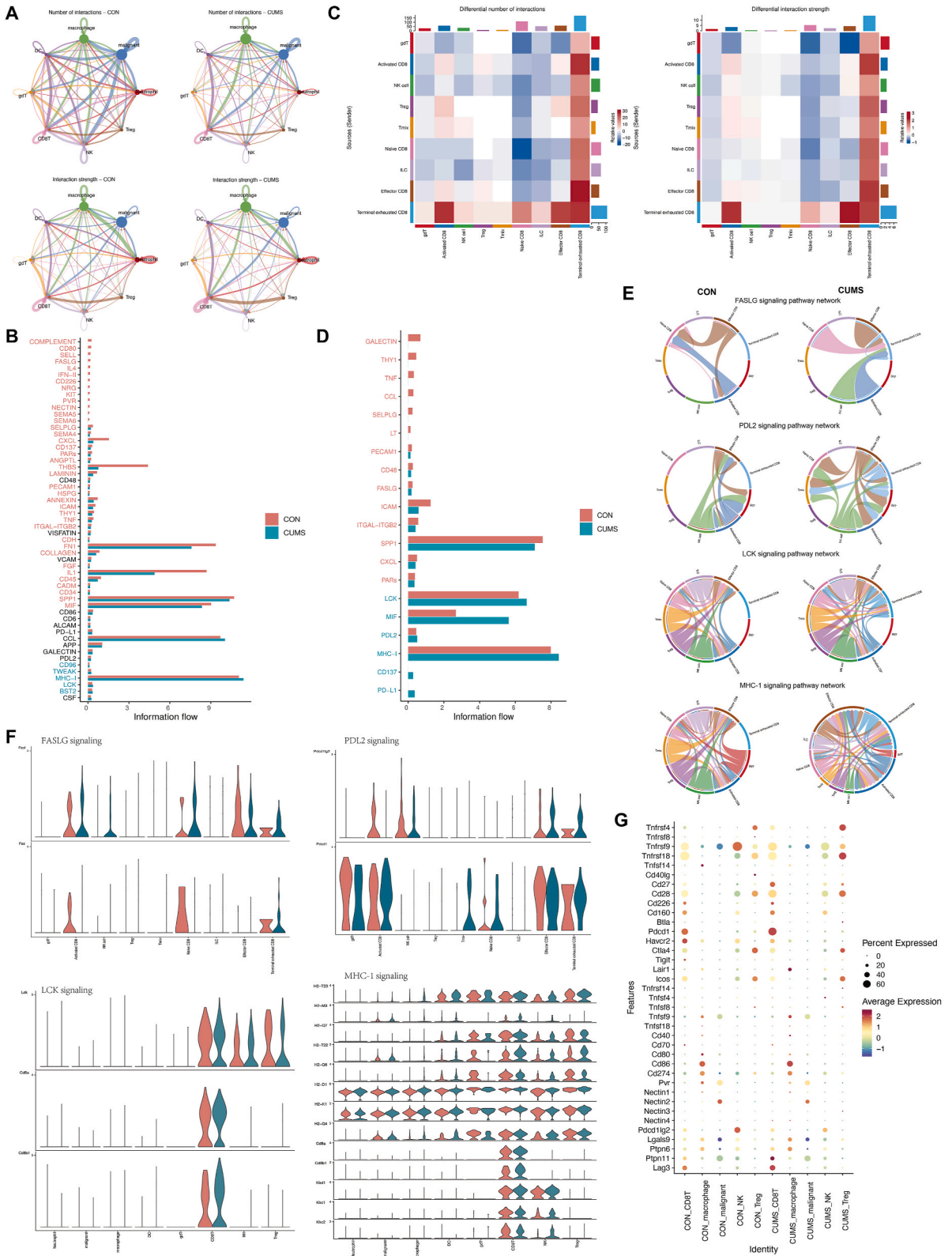


Fig. 6. Analysis of gdT cells. (A) Differences in gene expression between the control and CUMS groups. (B–C) GO enrichment analysis of gdT cells. (D) GO enrichment analysis of activated gdT cells.



(caption on next page)

Fig. 7. Cellular interactions in tumours. (A) Number and strength of cellular interactions in control and CUMS tumours. (B) The different information flows of signalling pathways in the two groups between cell types, including malignant cells, macrophages, CD8⁺ T cells, gdT cells, NK cells, neutrophils, and DCs. (C) Interactions of terminal exhausted CD8⁺ T cells in the two groups. (D) The different information flows of signalling pathways in the two groups between T-cell subsets. (E-F) Differential pathways and differential genes related to terminal exhausted CD8⁺ T cells between the two groups. (G) Expression of immune checkpoint proteins.

activity (Fig. S2A). The different genes of the effector CD8⁺ T-cell cluster in the CUMS group also exhibited immunosuppression and higher inflammation; notably, the downregulated genes in the CUMS group were enriched in Toll-like receptor signalling, which acts as the key molecule of innate immunity and a bridge connecting nonspecific immunity and specific immunity [26] (Fig. S2B). Tregs play an essential role in immune suppression and tolerance to promote CRC metastasis [27]. Gene enrichment in the CUMS group suggested decreased immune function of IL-17, TNF, and NOD-like receptor signalling (Fig. 5E), while the upregulated genes were involved in some mental disorders, such as Alzheimer’s disease, Parkinson’s disease, Huntington’s disease and retrograde endocannabinoid signalling (Fig. S2C), which revealed that chronic stress induces a large impact on Treg cells and plays an important role in CRC progression. In addition to the functional changes in different subtypes of T cells, immunohistochemical staining showed that the

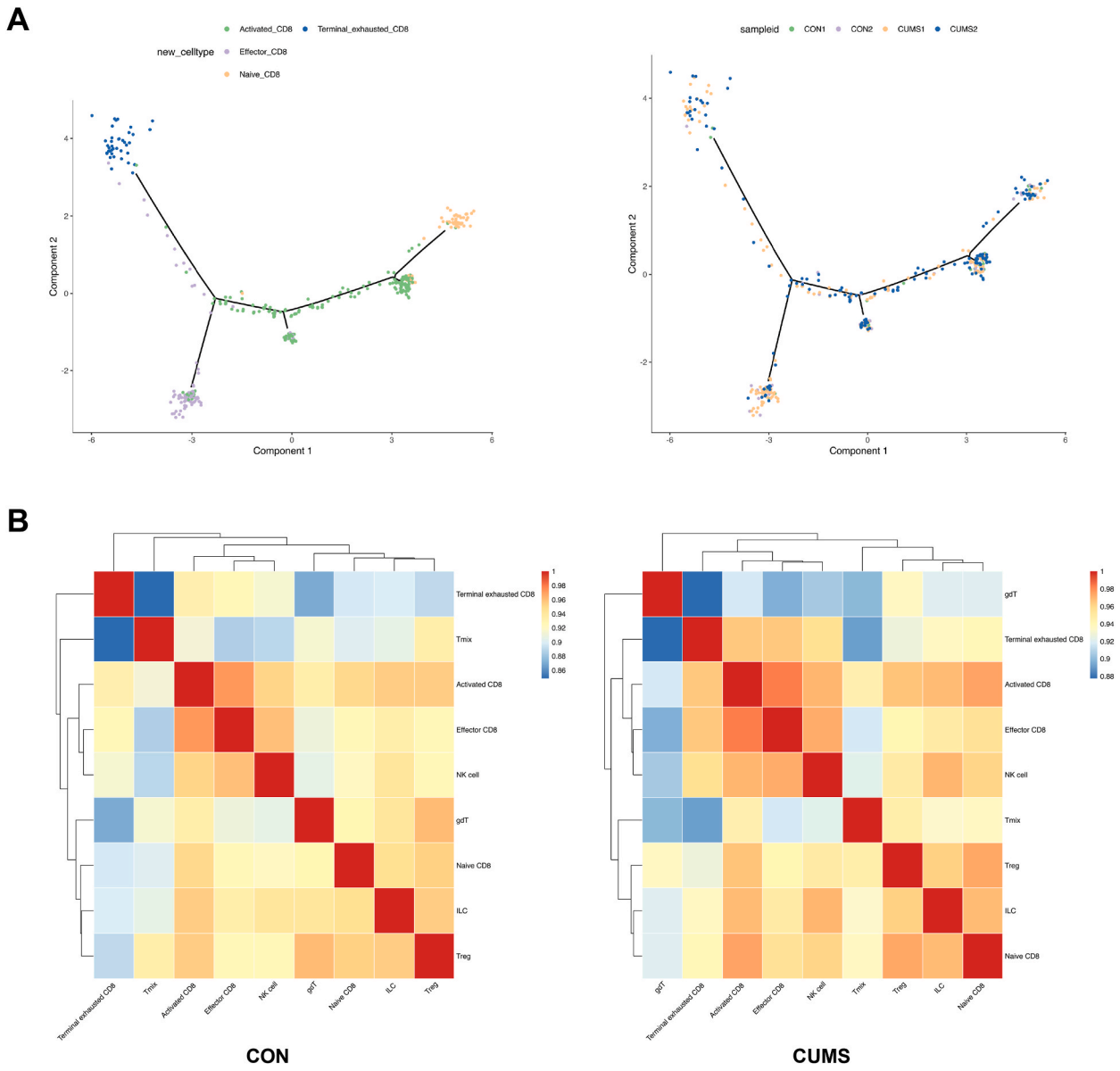


Fig. 8. Cellular interactions in tumours. (A) Pseudotime analysis of CD8⁺ T-cell subsets. (B) Correlation coefficient of gene expression between CD8⁺ T-cell subsets.

infiltration of T cells and CD8⁺ T cells was significantly reduced inside CUMS group tumours, and CD4⁺ T cells were increased in both the tumour margin and inside (Fig. 5F and G). Furthermore, we observed upregulated CCL8 in almost all adaptive immune T-cell subtypes in the CUMS group, which may be a target in the TIME for tumour progression under emotional stress (Fig. 5H).

Gamma delta T cells (gdT cells), the tumour infiltration of which has been shown to be associated with better prognoses in patients, are mainly distributed in mucous membranes and subcutaneous tissues, such as the intestinal tract, respiratory tract and genitourinary tract [28,29]. In the tumours of the CUMS group, the proportion of gdT cells was significantly reduced (Fig. 5C). The downregulated genes (Fig. 6A) were primarily concerned with the decrease in immune function, such as leukocyte aggregation, regulation of cytokine secretion involved in immune response, and activation-induced cell death of T cells, and were also associated with drug resistance, including cellular response to drug and drug binding (Fig. 6B). Conversely, functional enrichment analysis showed that the upregulated genes were primarily involved in inflammation, such as the positive regulation of my interleukins (IL-1, IL-18, IL-12, IL-2, and IL-6) and the positive regulation of the recognized inflammatory pathway NF- κ B signalling (Fig. 6C). KEGG enrichment analysis further revealed a strong association with depression-related cancer progression because the upregulated genes were involved in mental illness (Alzheimer's disease, Parkinson's disease, Huntington's disease) and cancer pathways (Fig. 6D). The above results suggest that both the proliferation and the antitumour function of gdT cells are inhibited in the tumours of the CUMS group.

2.5. Altered cellular interactions under CUMS-induced depression

To further elucidate the variations in the TIME under CUMS to reveal the mechanism by which depression promotes CRC progression, we inferred cellular interactions between different clusters by CellChat (Fig. S3D). Across all cell types identified, the number and strength of cell–cell interactions in the CUMS group were both reduced compared to controls (Fig. 7A and Fig. S3A), and we performed the differences in the information flow of signalling pathways between the two groups as well as differences in genes (Fig. 7B and Fig. S4). The analysis of the expression of immune checkpoints showed that CD8⁺ T cells in the CUMS group had higher expression of inhibitory immune checkpoints, including Pdc11, Ctla4, Ptpn6, Ptpn11 and Lag3 (Fig. 7G). Among T-cell subsets, the number and strength of interactions of terminally exhausted CD8⁺ T cells in the CUMS group were significantly increased (Fig. 7C). MHC-1 [30] and Lck [31] are key factors in the activation of T cells that are significantly upregulated in terminally exhausted CD8⁺ T cells under CUMS, as well as many other pathways, including the FASLG signalling pathway and PDL2 signalling pathway. Notably, PD-L1 information flow was detected only in the CUMS group (Fig. 7D–F and Figs. S5A and S5B).

Furthermore, combined with the previous gene analysis of T-cell subsets and the correlation analysis between lymphocyte subpopulations (Figs. 4B and 8B), we predicted that due to interference from the tumour microenvironment, effector T cells transformed into exhausted cells. Through pseudo-chronological analysis, we found that such cells do tend to transform into exhausted cells under chronic stress (Fig. 8A and Fig. 55C), which may be responsible for the poor prognosis in CRC.

3. Discussion

As the number of young cancer patients has increased, the mental health problems of these people have attracted much attention from researchers. A recent meta-analysis showed a significant association between CRC and depression. Particularly after diagnosis, patients with CRC are at significantly higher risk of developing depression than people without cancer, which impairs survival and quality of life [32]. Studies have shown that immunosuppressive acidic protein was positively correlated with depression scores in patients with advanced CRC, and in depressed CRC patients, the proportions of CD3⁺ and CD4⁺ lymphocytes were significantly lower than those in nondepressed patients [33]. The impact of psychological intervention on the side effects and immune function of colorectal cancer patients during treatment has attracted the attention of scientists, and corresponding clinical research is being carried out [34]. Mismatch repair-proficient (MMRp) tumours, including microsatellite stable (MSS) tumours or tumours with intact MMR proteins, which account for approximately 95 % of metastatic CRC, are unresponsive to immunotherapy [35]. Therefore, it is urgent to discover the immune evasion mechanism of CRC and develop new immunotherapy sites.

The immune system is divided into the innate immune system (nonspecific immunity) and the adaptive immune system (specific immunity) [36]. As the first line of defence against pathogen invasion, innate immunity is closely related to the inflammatory response, which can drive CRC progression [37]. The cells involved in the innate immune response mainly include phagocytic cells, macrophages, neutrophils, dendritic cells (DCs), and natural killer (NK) cells. One type of macrophage has an antitumour effect due to its intrinsic phagocytosis and antibody-dependent cell-mediated cytotoxicity (ADCC) bias towards the M1 phenotype [38], while tumour-associated macrophages (TAMs) tend to be the M2 phenotype and can promote angiogenesis and immune escape of tumour cells by secreting some anti-inflammatory cytokines and chemokines [39]. In tumours of the CUMS group, the increased M2 macrophage infiltration and decreased M1 macrophage infiltration exhibited a pronounced tumour-promoting effect (Fig. 4H). Similar to macrophages, many subtypes of neutrophils with different effects in the TIME have been identified. In the CUMS group, the antitumour subpopulation decreased and exhibited attenuated antitumour immunity (Fig. 3C–F). Innate lymphoid cells (ILCs), which are located on the surface of the intestinal mucosa, are able to respond quickly to fight pathogens in the first time when they invade, enhance intestinal immunity, and maintain homeostasis of intestinal mucosal immunity, and their proportion was reduced in the TIME of the CUMS group (Fig. 5C).

Innate immunity is a rapid immune mechanism of the body and can sculpt the TIME by regulating specific immunity [40]. Toll-like receptor plays a key role in communicating innate and adaptive immunity, and its signalling was downregulated in Activated and Effector CD8⁺ T cells of CUMS tumours, suggesting a weakened adaptive immune response (Fig. 5D and Fig. S2B). CD8⁺ T cells, also known as cytotoxic T cells, are one of the most important cells in antitumour immunity. Although their proportion slightly increased in

the tumours of the CUMS group, according to the correlation analysis and the pseudotime series analysis between the cell subsets (Fig. 8), we speculated that CD8⁺ T cells evolved into exhausted T cells, which may be the reason for the poor prognosis. In addition, CRC is often accompanied by intestinal inflammation. A reliable study has proven that CD8⁺ T cells are expanded in colitis patients, which is dynamically related to tissue-resident memory cells (Trms) [41], which suggests the particularity of the TIME of CRC. A study showed that CD8⁺ T effector memory cells with high expression of GZMK are associated with worse outcomes in CRC patients [42]. Interestingly, in our research, the identified T-cell subsets including Activated CD8⁺T cells, Effector CD8⁺T cells, Naive CD8⁺T cells, Terminal exhausted CD8⁺T cells, all highly expressed GZMK, and among them, Activated CD8⁺T cells, Naive CD8⁺T cells, Terminal exhausted CD8⁺T cells whose proportions increased in CUMS group tumours, also highly express CCR7(a marker of CD8⁺T central memory cells) (Fig. 5B and C), maybe it is also a factor in how depression promotes CRC progression.

Gamma delta T cells (gdT cells) distributed in the intestinal mucosa, skin and other mucosal tissues are recognized as the most potent immune cells in the human body [43,44]. gdT cells and NK cells have an effector-like program to sense and kill tumour cells [45]. However, in addition to some activating receptors, including NKG2D, NCR, CD16, DNAM-1 and death ligands, which commonly exist on NK cells, gdT cells can also use their unique ($\gamma\delta$) TCR to distinguish normal cells from cancer cells and then selectively kill cancer cells [46]. In the CUMS group, gdT cells exhibited a significantly reduced proportion and were closely related to mental diseases and immunosuppression (Figs. 5C and 6B and D), which deserves more in-depth research in CRC.

Overall, CUMS-induced depression shapes the immunosuppressive microenvironment of CRC to promote tumour progression and is involved in the dysregulation of immune cell infiltration, reduction of antitumour immune function, and weakening of cellular interactions. Further investigation is necessary due to the complexity of the crosstalk between the inherent immune system of the intestinal mucosa, the inflammatory environment closely related to CRC, and even the neuroendocrine system disorder caused by emotional disorders.

4. Materials and methods

4.1. Cell culture

The human CRC cell line CT26 purchased from the Chinese Academy of Sciences was cultured in RPMI 1640 medium (Corning, USA), which contained 10 % foetal bovine serum (Gibco Life Technologies, USA) and 1 % penicillin and streptomycin (Thermo Fisher Scientific, USA), and incubated in 5 % CO₂ in a 37 °C humidified incubator.

4.2. Animal models

Forty BALB/c mice were randomly divided into a control group and a CUMS group. Mice were modelled with CUMS from four weeks old and lasted for 2 months, including modified light/dark cycle, 24 h water/food deprivation, soiled bedding for 24 h, stroboscopic flashing lights of 2 times/s for 3 h, 1 min pinch at 1 cm from the tail end, 5 min swimming in 4 °C ice water, 3 h restraint, cage tilting at 45° from the horizontal for 24 h, etc. [47]. The stressors are randomly distributed during the modelling period and ensure that they are not repeated in the two days before and after. At the third week, 30 μ L of CT26 cell suspension was injected at a concentration of 1×10^8 cells/mL under the rectal mucosa of every mouse (Fig. 1 A). Before the mice were sacrificed, the open field test (OFT), tail suspension test (TST) and forced swimming test (FST) were performed to detect depression-like behaviour.

4.3. Open field test (OFT)

A well-lit and quiet place was chosen, and the mouse was placed in an instrument with a black bottom plate, white walls (50 cm \times 50 cm \times 50 cm), and an open upper part. The camera was placed 1.5 m above the centre so that the bottom of the open field was fully exposed to the screen. Each mouse was gently placed in the centre of the testing device, and the mouse activity was recorded for 5 min using software (SuperMaze, XR-XZ301, Shanghai Xinruan). After each mouse test, the bottom of the device was cleaned with low-concentration ethanol and dried with paper towels to avoid disturbing the next mouse test.

4.4. Tail suspension test (TST)

The rear 1/3 of the tail of the mouse was fixed with tape and hung on a stand with the head 20 cm away from the table. After adapting for 1 min, two different experimenters recorded the immobility time of the mouse within 5 min.

4.5. Forced swimming test (FST)

The mouse was gently placed into a cylindrical container (25 cm high \times 15 cm diameter) filled with sterilized grade pure water (water temperature 23 ± 1 °C). Mice were allowed to stay in the container for 6 min, and the last 5 min of immobility time was recorded by two different experimenters.

4.6. Single-cell suspension preparation

Fresh intestinal tumour tissues were harvested from mice with surgical scissors. Under sterile conditions, the cells were washed

twice with precooled RPMI 1640 medium. Then, the tissues were cut into small pieces of approximately 0.5 mm³, digested in an incubator shaker with enzymatic solution (Collagenase Type II, powder, Gibco, USA; pancreatin, Generay, China) at 37 °C for 60 min, and mixed by inverting every 5–10 min. After that, digested cell suspensions were filtered with 40 µm cell sieves, and then the cell pellets obtained after centrifugation were resuspended in an equal volume of erythrocyte lysate (Miltenyi, USA) for 10 min at 4 °C, centrifuged after red blood cells were lysed, and then washed once with 1 × PBS. Finally, the cell pellets were resuspended in the appropriate volume of medium, and the concentration and viability were determined with a cell counter (Bio-Rad, USA).

4.7. Single-cell encapsulation and library generation

The cell suspension was prepared at a concentration of 1 × 10⁶ cells/ml and encapsulated in a water-in-oil emulsion, and sequencing performance and library generation were performed according to the operation manual of 10 × Genomics (Cat. No. 1000268, USA). The constructed library was subjected to high-throughput sequencing with the Nova 6000 platform (Illumina, USA).

4.8. Dimensionality reduction and cluster analysis

We screened for highly variable genes using the FindClusters function in Seurat to perform graph-based clustering of cells based on their gene expression profiles. Finally, cells were visualized using a 2-dimensional uniform manifold approximation and projection (UMAP) algorithm with the RunUMAP function in Seurat.

4.9. Gene set variation analysis (GSVA) analysis

Background gene set files were first downloaded and organized from the KEGG database (<https://www.kegg.jp/>) via the GSEABase package (v1.44.0), and then pathway activity was performed on individual cells using the GSVA package [48] (v1.30.0). Finally, the LIMMA software package (v3.38.3) was used to evaluate the different activities of signalling pathways between the two groups.

4.10. GO and KEGG enrichment analysis

The GO and KEGG enrichment analysis between the two groups was performed by GSEA [49] using the C5 GO gene set and the C2 KEGG gene set (v7.2) in the MSigDB data.

4.11. CellChat cell communication analysis

The CellChat (v 1.1.3) R package [50] was used to analyse ligand–receptor interactions between cells. First, import the standardized expression matrix, create a cellChat object with the createCellChat function, and then use the default parameters to perform preprocessing operations with the identifyOverExpressedGenes identifyOverExpressedInteractions and projectData functions. Potential ligand–receptor interactions were calculated by the computeCommunProb, filterCommunication (min.cells = 10) and computeCommunProbPathway functions. Finally, the intercellular communication network is aggregated by the aggregateNet function.

4.12. Pseudotime analysis

We used the Monocle2 (v2.9.0) package [51] to infer cell differentiation trajectories. The specific steps are as follows: First, the importCDS function of the Monocle2 package was used to convert the Seurat object into a CellDataSet object, and the differentialGeneTest function was used to filter out the genes for cell sorting (ordering gene, qval < 0.01). Then, the reduceDimension function was used for dimensionality reduction clustering, and the differentiation trajectory was inferred by the orderCells function.

4.13. Haematoxylin-eosin staining

Tissues fixed in 4 % paraformaldehyde (Beyotime, China) were dehydrated and embedded to form tissue wax blocks, which were cut into slices with a thickness of 4 µm with a paraffin microtome (Leica, Germany). Paraffin sections were dipped into xylene twice for 20 min each, anhydrous ethanol twice for 5 min each, and 75 % ethanol to deparaffinize and rinse with tap water. Then, the sections were treated with haematoxylin differentiation solution (Servicebio, China) and rinsed with tap water. Following immersion in 85 % ethanol for 5 min and 95 % ethanol for 5 min, the sections were placed in eosin dye (Servicebio, China) for 5 min and then dehydrated. Finally, the slides were sealed with neutral gum (SCRC, China), observed and photographed under a microscope (Olympus, Japan).

4.14. Immunohistochemistry and immunofluorescence

The tissue sections were placed in a pressure cooker filled with citrate antigen retrieval buffer (Servicebio, China). After natural cooling, the slides were washed 3 times with PBS for 3 min each time. After serum blocking, sections were incubated with the following primary antibodies overnight at 4 °C: CD4 (GB13064-2, Servicebio) and CD8 (GB114196, Servicebio) to detect T cells; CD86 (19589S, CST) and CD206 (24595S, CST) to detect TAMs, washed 3 times with PBS, incubated with HRP-conjugated or fluorescently conjugated secondary antibodies at room temperature for 50 min, and labelled with DAPI (Beyotime, China). Finally, the slides were mounted

with neutral gum and observed, and pictures were taken under a fluorescence microscope (Leica, Germany).

4.15. Statistical analysis

Statistical analysis was conducted using GraphPad Prism 9.0 at the 95 % confidence level (GraphPad Software, USA). The statistical significance of two groups, including TST, FST and weights, was determined with a T test. $P < 0.05$ was considered a statistically significant difference.

Funding

National Natural Science Foundation of China (82122075). National Natural Science Foundation of China (82074232). Shanghai Frontier Research Base of Disease and Syndrome Biology of Inflammatory Cancer *Trans*-formation (2021KJ03-12). “Shu Guang” project supported by Shanghai Municipal Education Commission and Shanghai Education Development Foundation (21SG43).

Ethics statement

All the animal procedures were performed in accordance with the Guidelines for Care and Use of Laboratory Animals (Ministry of Health of the People’s Republic of China), and the experiments were approved by the Animal Ethics Committee of Shanghai (Ethics approval number: PZSHUTCM220913004). All animal studies complied with the ARRIVE guidelines.

Data availability statement

All data are available in the main text or the supplementary materials.

CRediT authorship contribution statement

Yingru Zhang: Writing - review & editing, Writing - original draft, Methodology, Investigation, Formal analysis, Data curation, Conceptualization. **Ying Feng:** Investigation. **Yiyang Zhao:** Investigation. **Yuanyuan Feng:** Investigation. **Mengyao Li:** Investigation. **Wenkai Wang:** Investigation. **Zhongya Ni:** Funding acquisition. **Huirong Zhu:** Funding acquisition. **Yan Wang:** Supervision, Project administration, Funding acquisition, Conceptualization.

Declaration of competing interest

The authors declare that they have no known competing financial interests or personal relationships that could have appeared to influence the work reported in this paper.

Acknowledgments

We thank OE Biotech Co., Ltd (Shanghai, China) for providing single-cell RNA-seq, Wenyang Ding, Zhuoya Zhang for assistance with bioinformatics analysis.

Appendix A. Supplementary data

Supplementary data to this article can be found online at <https://doi.org/10.1016/j.heliyon.2023.e23552>.

References

- [1] I. Arteaga Pérez, Emotion work during colorectal cancer treatments, *Med. Anthropol.* 41 (2022) 197–209.
- [2] M.L. Neuhouser, A.K. Aragaki, R.L. Prentice, J.E. Manson, R. Chlebowski, C.L. Carty, H.M. Ochs-Balcom, C.A. Thomson, B.J. Caan, L.F. Tinker, R.P. Urrutia, J. Knudtson, G.L. Anderson, Overweight, obesity, and postmenopausal invasive breast cancer risk: a secondary analysis of the women’s health initiative randomized clinical trials, *JAMA Oncol.* 1 (2015) 611–621.
- [3] S. Brandhorst, I.Y. Choi, M. Wei, C.W. Cheng, S. Sedrakyan, G. Navarrete, L. Dubeau, L.P. Yap, R. Park, M. Vinciguerra, S. Di Biase, H. Mirzaei, M.G. Mirisola, P. Childress, L. Ji, S. Groshen, F. Penna, P. Odetti, L. Perin, P.S. Conti, Y. Ikeno, B.K. Kennedy, P. Cohen, T.E. Morgan, T.B. Dorff, V.D. Longo, A periodic diet that mimics fasting promotes multi-system regeneration, enhanced cognitive performance, and healthspan, *Cell Metabol.* 22 (2015) 86–99.
- [4] K.M. Di Sebastiano, G. Murthy, K.L. Campbell, S. Desroches, R.A. Murphy, Nutrition and cancer prevention: why is the evidence lost in translation? *Adv. Nutr.* 10 (2019) 410–418.
- [5] O.I. Okereke, C.M. Vyas, D. Mischoulon, G. Chang, N.R. Cook, A. Weinberg, V. Bubes, T. Copeland, G. Friedenberg, I.M. Lee, J.E. Buring, C.F. Reynolds, J. E. Manson, Effect of long-term supplementation with marine omega-3 fatty acids vs placebo on risk of depression or clinically relevant depressive symptoms and on change in mood scores: a randomized clinical trial, *JAMA* 326 (2021) 2385–2394.
- [6] O.I. Okereke, C.F. Reynolds, D. Mischoulon, G. Chang, C.M. Vyas, N.R. Cook, A. Weinberg, V. Bubes, T. Copeland, G. Friedenberg, I.M. Lee, J.E. Buring, J. E. Manson, Effect of long-term vitamin D3 supplementation vs placebo on risk of depression or clinically relevant depressive symptoms and on change in mood scores: a randomized clinical trial, *JAMA* 324 (2020) 471–480.

- [7] S. Baziliansky, M. Cohen, Emotion regulation patterns among colorectal cancer survivors: clustering and associations with personal coping resources, *Behav. Med.* 47 (2021) 214–224.
- [8] R. Jia, N. Liu, G. Cai, Y. Zhang, H. Xiao, L. Zhou, Q. Ji, L. Zhao, P. Zeng, H. Liu, J. Huo, X. Yue, Y. Zhang, C. Wu, X. Sun, Y. Feng, H. Liu, H. Liu, Z. Han, Y. Lai, Y. Zhang, G. Han, H. Gong, Y. Wang, Q. Li, Effect of PRM1201 combined with adjuvant chemotherapy on preventing recurrence and metastasis of stage III colon cancer: a randomized, double-blind, placebo-controlled clinical trial, *Front. Oncol.* 11 (2021), 618793.
- [9] G. Ostuzzi, F. Matcham, S. Dauchy, C. Barbui, M. Hotopt, Antidepressants for the Treatment of Depression in People with Cancer, *Cochrane Database Syst Rev*, 2015, p. CD011006.
- [10] J.R. Satin, W. Linden, M.J. Phillips, Depression as a predictor of disease progression and mortality in cancer patients: a meta-analysis, *Cancer* 115 (2009) 5349–5361.
- [11] J. Walker, A. Mulick, N. Magill, S. Symeonides, C. Gourley, K. Burke, A. Belot, M. Quartagno, M. van Niekerk, M. Toynbee, C. Frost, M. Sharpe, Major depression and survival in people with cancer, *Psychosom. Med.* 83 (2021) 410–416.
- [12] G. Buccafusca, I. Proserpio, A.C. Tralongo, S. Rametta Giuliano, P. Tralongo, Early colorectal cancer: diagnosis, treatment and survivorship care, *Crit. Rev. Oncol. Hematol.* 136 (2019) 20–30.
- [13] E.M.V. Reiche, S.O.V. Nunes, H.K. Morimoto, Stress, depression, the immune system, and cancer, *Lancet Oncol.* 5 (2004) 617–625.
- [14] M. Bekkbat, P.A. Howell, S.A. Rowson, S.D. Kelly, M.G. Tansey, G.N. Neigh, Chronic adolescent stress sex-specifically alters central and peripheral neuro-immune reactivity in rats, *Brain Behav. Immun.* 76 (2019) 248–257.
- [15] J.P. Lopez, E. Brivio, A. Santambrogio, C. De Donno, A. Kos, M. Peters, N. Rost, D. Czamara, T.M. Brückl, S. Roeh, M.L. Pöhlmann, C. Engelhardt, A. Ressler, R. Stoffel, A. Tontsch, J.M. Villamizar, M. Reincke, A. Riestler, S. Sbiera, M. Fassnacht, H.S. Mayberg, W.E. Craighead, B.W. Dunlop, C.B. Nemeroff, M. V. Schmidt, F.B. Binder, F.J. Theis, F. Beuschlein, C.L. Andoniadou, A. Chen, Single-cell molecular profiling of all three components of the HPA axis reveals adrenal ABCB1 as a regulator of stress adaptation, *Sci. Adv.* 7 (2021).
- [16] P.T. Rudak, J. Choi, K.M. Parkins, K.L. Summers, D.N. Jackson, P.J. Foster, A.I. Skaro, K. Leslie, V.C. McAlister, V.K. Kuchroo, W. Inoue, O. Lantz, S.M. M. Haeryfar, Chronic stress physically spares but functionally impairs innate-like invariant T cells, *Cell Rep.* 35 (2021), 108979.
- [17] H. Yang, L. Xia, J. Chen, S. Zhang, V. Martin, Q. Li, S. Lin, J. Chen, J. Calmette, M. Lu, L. Fu, J. Yang, Z. Pan, K. Yu, J. He, E. Morand, G. Schlecht-Louf, R. Krzysiek, L. Zitvogel, B. Kang, Z. Zhang, A. Leader, P. Zhou, L. Lanfumey, M. Shi, G. Kroemer, Y. Ma, Stress-glucocorticoid-TSC2D23 axis compromises therapy-induced antitumor immunity, *Nat. Med.* 25 (2019) 1428–1441.
- [18] P. See, J. Lum, J. Chen, F. Ginhoux, A single-cell sequencing guide for immunologists, *Front. Immunol.* 9 (2018) 2425.
- [19] C. Suo, E. Dann, I. Goh, L. Jardine, V. Kleshchevnikov, J.-E. Park, R.A. Botting, E. Stephenson, J. Engelbert, Z.K. Tuong, K. Polanski, N. Yayon, C. Xu, O. Suchanek, R. Elmentaita, C. Dominguez Conde, P. He, S. Pritchard, M. Miah, C. Moldovan, A.S. Steemers, P. Mazin, M. Prete, D. Horsfall, J.C. Marioni, M. R. Clatworthy, M. Haniffa, S.A. Teichmann, Mapping the Developing Human Immune System across Organs, *Science*, New York, N.Y., 2022, p. 376, eabo0510.
- [20] M.L. Wikberg, A. Ling, X. Li, Å. Öberg, S. Edin, R. Palmqvist, Neutrophil infiltration is a favorable prognostic factor in early stages of colon cancer, *Hum. Pathol.* 68 (2017) 193–202.
- [21] V. Governa, E. Trella, V. Mele, L. Tornillo, F. Amicarella, E. Cremonesi, M.G. Muraro, H. Xu, R. Droseser, S.R. Däster, M. Bolli, R. Rosso, D. Oertli, S. Eppenberger-Castori, L.M. Terracciano, G. Iezzi, G.C. Spagnoli, The interplay between neutrophils and CD8 T cells improves survival in human colorectal cancer, *Clin. Cancer Res.* 23 (2017) 3847–3858.
- [22] L. Wang, Y. Liu, Y. Dai, X. Tang, T. Yin, C. Wang, T. Wang, L. Dong, M. Shi, J. Qin, M. Xue, Y. Cao, J. Liu, P. Liu, J. Huang, C. Wen, J. Zhang, Z. Xu, F. Bai, X. Deng, C. Peng, H. Chen, L. Jiang, S. Chen, B. Shen, Single-cell RNA-seq analysis reveals BHLHE40-driven pro-tumour neutrophils with hyperactivated glycolysis in pancreatic tumour microenvironment, *Gut* (2022).
- [23] A. Butler, P. Hoffman, P. Smibert, E. Papalexli, R. Satija, Integrating single-cell transcriptomic data across different conditions, technologies, and species, *Nat. Biotechnol.* 36 (2018) 411–420.
- [24] R. Xue, Q. Zhang, Q. Cao, R. Kong, X. Xiang, H. Liu, M. Feng, F. Wang, J. Cheng, Z. Li, Q. Zhan, M. Deng, J. Zhu, Z. Zhang, N. Zhang, Liver tumour immune microenvironment subtypes and neutrophil heterogeneity, *Nature* 612 (2022) 141–147.
- [25] N. Müller, M.J. Schwarz, The immune-mediated alteration of serotonin and glutamate: towards an integrated view of depression, *Mol. Psychiatr.* 12 (2007).
- [26] D. Li, M. Wu, Pattern recognition receptors in health and diseases, *Signal Transduct. Targeted Ther.* 6 (2021) 291.
- [27] J.C. Lee, S. Mehdizadeh, J. Smith, A. Young, I.A. Mufazalov, C.T. Mowery, A. Daud, J.A. Bluestone, Regulatory T cell control of systemic immunity and immunotherapy response in liver metastasis, *Sci Immunol* 5 (2020).
- [28] F. Zhong, Y. Lin, X. Jing, Y. Ye, S. Wang, Z. Shen, Innate tumor killers in colorectal cancer, *Cancer Lett.* 527 (2022) 115–126.
- [29] Z. Sebestyen, I. Prinz, J. Déchanet-Merville, B. Silva-Santos, J. Kuball, Translating gammadelta ($\gamma\delta$) T cells and their receptors into cancer cell therapies, *Nat. Rev. Drug Discov.* 19 (2020) 169–184.
- [30] E.J. Brea, C.Y. Oh, E. Manchado, S. Budhu, R.S. Gejman, G. Mo, P. Mondello, J.E. Han, C.A. Jarvis, D. Ulmert, Q. Xiang, A.Y. Chang, R.J. Garippa, T. Merghoub, J.D. Wolchok, N. Rosen, S.W. Lowe, D.A. Scheinberg, Kinase regulation of human MHC class I molecule expression on cancer cells, *Cancer Immunol. Res.* 4 (2016) 936–947.
- [31] F.A. Hartl, E. Beck-Garcia, N.M. Woessner, L.J. Flachsmann, R.M.H.V. Cárdenas, S.M. Brandl, S. Taromi, G.J. Fiala, A. Morath, P. Mishra, O.S. Yousefi, J. Zimmermann, N. Hoeflin, M. Köhn, B.M. Wöhr, R. Zeiser, K. Schweimer, S. Günther, W.W. Schamel, S. Minguet, Author Correction: noncanonical binding of Lck to CD3 ϵ promotes TCR signaling and CAR function, *Nat. Immunol.* 22 (2021) 100–101.
- [32] V. Cheng, N. Oveis, H. McTaggart-Cowan, J.M. Loree, R.A. Murphy, M.A. De Vera, Colorectal cancer and onset of anxiety and depression: a systematic review and meta-analysis, *Curr. Oncol.* 29 (2022) 8751–8766.
- [33] R. Li, J. Yang, J. Yang, W. Fu, H. Jiang, J. Du, C. Zhang, H. Xi, J. Hou, Depression in older patients with advanced colorectal cancer is closely connected with immunosuppressive acidic protein, *Metab. Brain Dis.* 29 (2014) 87–92.
- [34] M. Wang, Y. Xu, J. Shi, C. Zhuang, Y. Zhuang, J. Li, P.H. Cashin, The effect of cognitive behavioral therapy on chemotherapy-induced side effects and immune function in colorectal cancer patients undergoing chemotherapy: study protocol for a randomized controlled trial, *J. Gastrointest. Oncol.* 14 (2023) 1869–1877.
- [35] R. Cohen, B. Rousseau, J. Vidal, R. Colle, L.A. Diaz, T. André, Immune checkpoint inhibition in colorectal cancer: microsatellite instability and beyond, *Targeted Oncol.* 15 (2020) 11–24.
- [36] K.A. Deets, R.E. Vance, Inflammasomes and adaptive immune responses, *Nat. Immunol.* 22 (2021) 412–422.
- [37] X. Yu, D. Wang, X. Wang, S. Sun, Y. Zhang, S. Wang, R. Miao, X. Xu, X. Qu, CXCL12/CXCR4 promotes inflammation-driven colorectal cancer progression through activation of RhoA signaling by sponging miR-133a-3p, *J. Exp. Clin. Cancer Res.* 38 (2019) 32.
- [38] Y. Zhang, Y. Zhao, Q. Li, Y. Wang, Macrophages, as a promising strategy to targeted treatment for colorectal cancer metastasis in tumor immune microenvironment, *Front. Immunol.* 12 (2021), 685978.
- [39] C. Liu, Z. Yao, J. Wang, W. Zhang, Y. Yang, Y. Zhang, X. Qu, Y. Zhu, J. Zou, S. Peng, Y. Zhao, S. Zhao, B. He, Q. Mi, X. Liu, X. Zhang, Q. Du, Macrophage-derived CCL5 facilitates immune escape of colorectal cancer cells via the p65/STAT3-CSN5-PD-L1 pathway, *Cell Death Differ.* 27 (2020) 1765–1781.
- [40] D.C. Hinshaw, L.A. Shevde, The tumor microenvironment innately modulates cancer progression, *Cancer Res.* 79 (2019) 4557–4566.
- [41] A.M. Luoma, S. Suo, H.L. Williams, T. Sharova, K. Sullivan, M. Manos, P. Bowling, F.S. Hodi, O. Rahma, R.J. Sullivan, G.M. Boland, J.A. Nowak, S.K. Dougan, M. Dougan, G.-C. Yuan, K.W. Wucherpfennig, Molecular pathways of colon inflammation induced by cancer immunotherapy, *Cell* (2020) 182.
- [42] S. Tiberti, C. Catozzi, O. Croci, M. Ballerini, D. Cagnina, C. Soriani, C. Scirgolea, Z. Gong, J. He, A.D. Macandog, A. Nabinejad, C.B. Nava Lauson, A. Quinte, G. Bertalot, W.L. Petz, S.P. Ravenda, V. Licursi, P. Paci, M. Rasponi, L. Rotta, N. Fazio, G. Ren, U. Fumagalli-Romario, M.H. Schaefer, S. Campaner, E. Lugli, L. Nezi, T. Manzo, Author Correction: GZMK CD8 T effector memory cells are associated with CD15 neutrophil abundance in non-metastatic colorectal tumors and predict poor clinical outcome, *Nat. Commun.* 13 (2022) 7380.
- [43] V. Groh, A. Steinle, S. Bauer, T. Spies, Recognition of stress-induced MHC molecules by intestinal epithelial gammadelta T cells, *Science* (New York, N.Y.) 279 (1998) 1737–1740.

- [44] P.A. Duya, Y. Chen, L. Bai, Z. Li, J. Li, R. Chai, Y. Bian, S. Zhao, Nature products of traditional Chinese medicine provide new ideas in $\gamma\delta$ T cell for tumor immunotherapy, *Acupuncture and Herbal Medicine* 2 (2022) 78–83.
- [45] S.-R. Woo, L. Corrales, T.F. Gajewski, Innate immune recognition of cancer, *Annu. Rev. Immunol.* 33 (2015) 445–474.
- [46] B. Silva-Santos, K. Serre, H. Norell, $\gamma\delta$ T cells in cancer, *Nat. Rev. Immunol.* 15 (2015) 683–691.
- [47] S. Antoniuk, M. Bijata, E. Ponimaskin, J. Włodarczyk, Chronic unpredictable mild stress for modeling depression in rodents: meta-analysis of model reliability, *Neurosci. Biobehav. Rev.* 99 (2019) 101–116.
- [48] S. Hänzelmann, R. Castelo, J. Guinney, GSEA: gene set variation analysis for microarray and RNA-seq data, *BMC Bioinf.* 14 (2013) 7.
- [49] A. Subramanian, P. Tamayo, V.K. Mootha, S. Mukherjee, B.L. Ebert, M.A. Gillette, A. Paulovich, S.L. Pomeroy, T.R. Golub, E.S. Lander, J.P. Mesirov, Gene set enrichment analysis: a knowledge-based approach for interpreting genome-wide expression profiles, *P Natl Acad Sci USA* 102 (2005) 15545–15550.
- [50] S. Jin, C.F. Guerrero-Juarez, L. Zhang, I. Chang, R. Ramos, C.-H. Kuan, P. Myung, M.V. Plikus, Q. Nie, Inference and analysis of cell-cell communication using CellChat, *Nat. Commun.* 12 (2021) 1088.
- [51] C. Trapnell, D. Cacchiarelli, J. Grimsby, P. Pokharel, S. Li, M. Morse, N.J. Lennon, K.J. Livak, T.S. Mikkelsen, J.L. Rinn, The dynamics and regulators of cell fate decisions are revealed by pseudotemporal ordering of single cells, *Nat. Biotechnol.* 32 (2014) 381–386.